

Pulsed-laser-deposited ultraviolet-emitting SrS:Te thin films

J. M. Fitz-Gerald^{a)} and J. Hoekstra

Department of Materials Science and Engineering, University of Virginia, Charlottesville, Virginia 22904-4745

P. D. Rack and J. D. Fowlkes

Department of Materials Science and Engineering, University of Tennessee, Knoxville, Tennessee 37996-2200

(Received 17 January 2003; accepted 12 March 2003)

SrS has an indirect band gap of ~ 4.32 eV, however, when it is doped with tellurium, ultraviolet emission occurs at 360 nm and 400 nm due to recombination from bound exciton states. In this letter, we discuss the ultraviolet emission of pulsed-laser-deposited thin films of SrS:Te grown at room temperature on Si. The deposited film thickness ranged from 0.1–1.5 μm , with optimized films grown at ~ 0.5 μm . Te doping was incorporated by both ion implantation and conventional diffusion of deposited Te films. The characteristics of the ultraviolet emission will be discussed and correlated to the microstructural, chemical, and optical properties of the films. © 2003 American Institute of Physics. [DOI: 10.1063/1.1571660]

The development of semiconductor-based ultraviolet (UV) light sources is of critical importance for miniaturized UV light sources, which have application in biological agent detection, nonlinear-of-sight covert communications, water purification, equipment/personnel decontamination, and white-light generation. Currently, a significant amount of research is being performed to extend the III–V nitride blue lasers and light-emitting diodes into the ultraviolet region. In this letter, we will discuss preliminary work (on SrS:Te) investigating tellurium-doped alkaline earth sulfide materials (SrS:Te, CaS:Te, and MgS:Te) as an alternative material for UV and deep UV solid-state light sources.

The theory of isoelectronic bound exciton emission was introduced by Thomas *et al.*^{1,2} in 1965 when they used this theory to describe the photoluminescence (PL) observed in GaP:N. They suggested that even though nitrogen has the same valence as phosphorus, nitrogen acts as an electron trap in the GaP lattice because nitrogen is significantly more electronegative than phosphorus. Consequently, electrons are preferentially trapped at nitrogen sites, which sets up a short-range Coulombic attraction for holes. Finally, when the hole is trapped, the electron and hole couple and form a bound exciton. The localization of the bound exciton causes the momentum to be diffuse (due to the uncertainty principle) and efficient radiation is realized in GaP, which has an indirect band gap. Since this model was suggested, the luminescent properties of other III–V, II–VI, and I–VII materials have been described by it.

For MS:Te semiconductors ($M = \text{Zn},^{3-6} \text{Cd},^{7-11} \text{Ba},^{12}$ and Sr),^{13,14} the bound exciton formation is similar to the GaP:N system except that the sulfur host anions have a larger electronegativity than the tellurium dopant. Consequently, holes are trapped at tellurium sites forming a tellurium–hole complex, which subsequently induces a Coulombic attraction for electrons. When the electron is trapped at this complex, the bound exciton is formed.

Rack *et al.* investigated the blue emission in BaS:Te¹² and thoroughly characterized the ultraviolet emission in

SrS:Te powder materials.^{13,14} In both cases, efficient PL from Te_S and $\text{Te}_S\text{-Te}_S$ was observed. SrS:Te powders were synthesized and found to have two high-energy emission bands with peak wavelengths at 360 and 400 nm. The 360 nm emission band dominated at lower tellurium concentrations and was attributed to Te_S bound excitons, whereas the 400 nm band dominated at higher tellurium concentrations and was ascribed to $\text{Te}_S\text{-Te}_S$ bound excitons.

All of the films for this research were deposited at room temperature using a pulsed excimer laser ($\lambda = 248$ nm) operating at 10 Hz with a 25 ns pulse [full width at half maximum (FWHM)]. A base pressure of 3×10^{-6} Torr was used for all experiments, while depositions were carried out in Ar and H_2S at pressures ranging from 50–200 mTorr. Films were grown on (100) single crystal *p*-type Si substrates. A high-purity pressed and sintered powder SrS sputtering target was used to deposit the bulk thin films, while a metallic Te sputtering target was used to deposit thin layers of Te. The excimer laser was incident on the target surface at a 45° angle with a resulting spot area of ~ 0.186 cm^2 for the bulk SrS thin films and 0.15 cm^2 for the Te thin-film layers. The optimized deposition fluence was found to be 1.6 J/cm^2 for the SrS bulk thin films and 1.0 J/cm^2 for the Te thin-film layers. A computer controlled scanning mirror was used to control laser beam movement over the surface of the target during deposition. Deposition rates for the SrS thin films were 5.3 Å/pulse while a deposition rate of 1.1 Å/pulse was used to deposit Te thin films onto the bulk SrS thin films for doping. In the initial study, three ~ 0.5 μm SrS films deposited on Si were implanted with Te^{++} . Doses of 5×10^{12} , 5×10^{13} , and 5×10^{14} atoms/ cm^2 were implanted at 150 kV which yields Te concentrations on the order of 1×10^{17} , 1×10^{18} , and 1×10^{19} atoms/ cm^3 , respectively, subsequent to the postimplant drive in and activation anneal. Another set of 0.5 μm films were capped with Te by pulsed laser deposition (PLD) with ~ 5.5 , 11, 16.5, and 22 Å of Te (i.e. 5, 10, 15, and 20 pulses), which should yield concentrations of $\sim 3.7 \times 10^{19}$, 7.4×10^{19} , 1.1×10^{20} , and 1.5×10^{20} atoms/ cm^3 , respectively. All samples were annealed at 850 °C in Ar for 3 h

^{a)}Electronic mail: jmf8h@virginia.edu

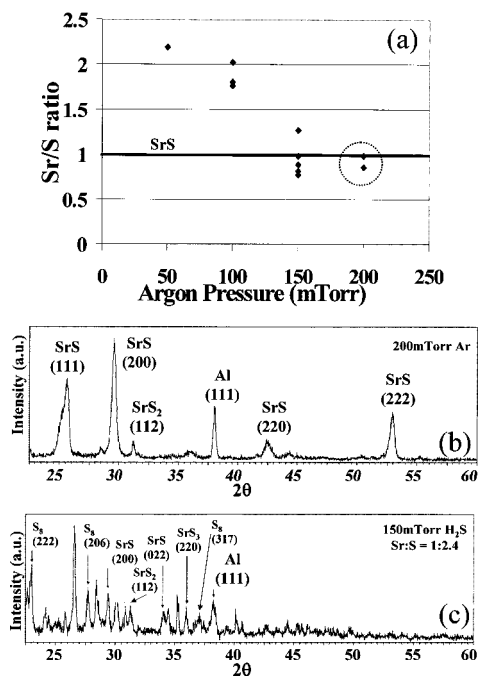


FIG. 1. (a) EDS Sr/S ratio as a function of background pressure. Representative as-deposited XRD patterns for SrS films grown in (b) Ar and (c) H₂S.

and were capped with another SrS thin film to minimize sulfur outgassing during annealing.

Thin-film characterization was performed with using a JEOL 6700F scanning electron microscope equipped with an energy dispersive spectrometer (EDS) and a fully integrated cathodoluminescence (CL) system equipped with imaging and scanning monochromator (0.2 nm resolution, 185–900 nm). All CL spectra were taken with a 1 s dwell time and a 2 nm scan step. X-ray diffraction (XRD) was performed using a Phillips X-pert x-ray diffractometer.

Initial investigations into the SrS:Te system have been conducted to establish the efficacy surrounding the use of PLD to grow thin films (0.1–1.5 μm) of SrS with controlled stoichiometry. For these experiments, thin films of SrS were grown in both Ar and H₂S atmospheres at room temperature with laser energy densities ranging from 1.5–2.1 J/cm². The Ar pressure was varied from 50–200 mTorr and it was clear from EDS and XRD that depositions performed at room temperature with a backfill atmosphere of 200 mTorr Ar produced the most accurate stoichiometry, 1:1 ratio of Sr to S as shown in Figs. 1(a) and 1(b). Thin-film SrS depositions performed at room temperature in a H₂S atmosphere produced thin films with a large amount of secondary SrS (with S/Sr ratio >1) and S complexes as shown in Fig. 1(c). This overpressure of S resulted in a Sr:S ratio of 1:2.4 as measured by EDS. By controlling the energy density and the growth time (i.e., 4000 pulses) for the films deposited in Ar at 200 mTorr, thin films were optimized for a thickness of 0.5 μm in Ar.

After the activation/drive-in anneal, some cracking and delamination of the SrS:Te films were observed. A previous investigation of the stresses in sputter deposited SrS showed that significant tensile stresses develop in the SrS films deposited on Si because of the large difference in the coefficient of thermal expansion of Si (4×10^{-6}) and SrS (25×10^{-6}).¹⁵ While the original stress state of the as-deposited films were not known, an estimate of the thermal stresses

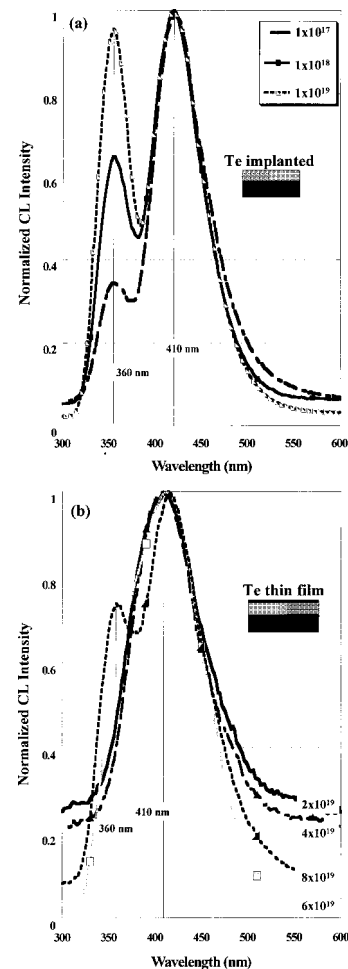


FIG. 2. CL measurements taken at 15 kV for both implanted (a), and Te capped films (b).

generated in the SrS:Te films during the cool down to 850 °C to room temperature is ~ 750 MPa in tension. XRD data from annealed samples showed a reduction in the FWHM.

An analysis of the specific postanneal dopant distribution has not been performed, however normalized CL spectra (taken at 15 keV) of the Te-implanted [Fig. 2(a)] and Te-doped thin films [Fig. 2(b)] showed emission from the signature Te_S and Te_S–Te_S bound exciton peaks at ~ 360 and 410 nm, respectively. Both sets of films in Fig. 2 show a counterintuitive trend in the peak ratio of the two peaks; namely that the Te_S peak height increases relative to the Te_S–Te_S peak height with increasing dopant concentration. It was expected that with increasing the dopant concentration the Te_S–Te_S emission peak would systematically increase because the probability of forming Te_S–Te_S increases with the Te concentration. The observed trends indicate that the Te dopant is not fully driven into the sample and a Te concentration gradient through the SrS thickness exists. Thus, the Te_S–Te_S pairs are spatially located in the near-surface region and the Te_S sites are located near the SrS–Si interface. Samples with the highest Te concentration have the largest concentration gradient thereby enhancing diffusion and creating more singlets at the SrS–Si interface. The enhanced Te_S bound exciton emission at higher dopant concentration is observed in Figure 2 with the highest Te_S emission coming from the highest doped samples ($\sim 1 \times 10^{19}$ and 1.5×10^{20} Te/cm³).

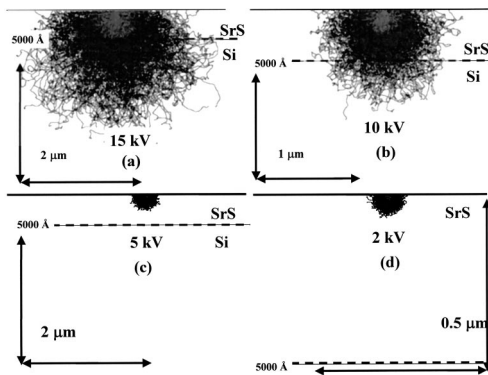


FIG. 3. Monte Carlo simulations of electron penetration depth as a function of beam energy for (a) 15 kV, (b) 10 kV, (c) 5 kV, and (d) 2 kV. It is clear from the lines representing the SrS/Si interface that the optimum beam energy for (5000 Å) thick films is between 7–10 kV.

The optimization of the beam interaction volume will also have a significant effect on the Te_S and $\text{Te}_S\text{--Te}_S$ emission. Figure 3 shows the Monte Carlo simulations of the electron penetration into the SrS/Si stack as a function of beam energy. The simulations show that the optimum beam energy is between 7–10 kV, with higher energies (>10 kV) penetrating into the underlying Si substrate and lower energies (<5–7 kV) failing to excite the complete volume of the SrS film. In addition, the Te_S bound exciton emission is anomalously high; however the electron–hole pairs are preferentially generated at the tail of the electron-beam distribution which has better overlap with the Te_S singlets distributed deeper into the film.

Figure 4 shows the CL intensity as a function of beam energy at 1, 5, 10, and 15 kV, respectively, for the highest doped ion implanted sample (Te concentration = 1×10^{19} atoms/cm³). The strongest CL emission is observed at 10 kV, confirming the simulations as a function of beam penetration depth. Another observation that must be noted is the shift of the singlet–doublet peak intensities at 15 kV between Figs. 3 and 4 for the same sample. The CL spectra in Fig. 4 was acquired with a $500\times$ image resolution at a faster beam scan rate ($75\times$), while the CL spectra shown in Fig. 3 were taken at $1000\times$ with a slow beam scan rate. It is speculated that along with the tellurium diffusion gradient, that several processes such as charging, current saturation, radiative and nonradiative energy transfer, internal electric-field gradients, and carbon staining, are occurring which are affecting both the Te_S singlet and $\text{Te}_S\text{--Te}_S$ doublet bound exciton emission. Detailed CL studies as well as complimentary PL studies are being performed to elucidate the dominant processes.

In summary, SrS:Te thin films were pulsed laser deposited in an argon atmosphere and their luminescent properties were investigated. Te doping was performed by both ion implantation and Te capping layers deposited by PLD. Samples were annealed in Ar at 850 °C for 3 hours. CL measurements taken at room temperature show characteristic Te_S and $\text{Te}_S\text{--Te}_S$ bound exciton emission at 360 nm, and 410–420 nm respectively, which is in excellent agreement with previous research efforts in SrS:Te powders at room temperature. The strong emission of $\text{Te}_S\text{--Te}_S$ (420 nm) at low doping

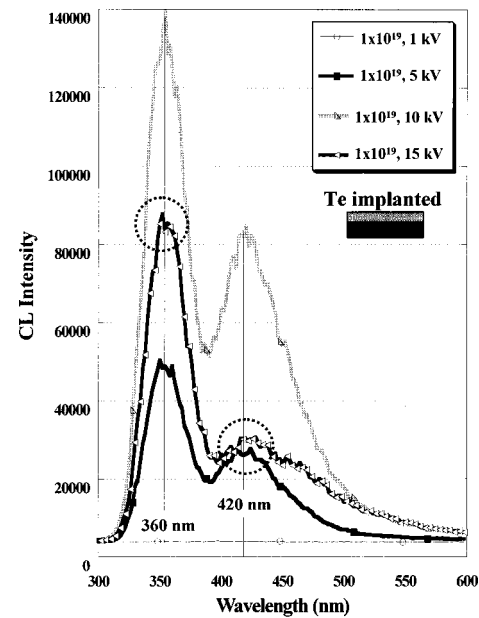


FIG. 4. CL intensity (not normalized) measured as a function of beam energy. Beam energies were varied from 1–15 kV showing the strongest CL emission at 10 kV, which is predicted by the Monte Carlo simulations.

concentrations and a rise in the emission of Te_S (360 nm) at high Te concentrations is counterintuitive to prior research investigations suggesting that there is a gradient in the Te dopant concentration through the films. This trend is present in both sets of thin films and is particularly noticeable for the highest-doped films. Beam energy CL measurements were varied from 1–15 kV on a heavily doped sample confirming simulations of the beam interaction volume in terms of CL emission.

The authors would like to acknowledge Dr. Chris Wette-land for ion implantations performed at Los Alamos National Laboratory and financial support from the AFOSR under DURINT equipment Grant No. F49620-01-1-0420.

- ¹D. G. Thomas, J. J. Hopfield, and C. J. Frosch, *Phys. Rev. B* **5**, 857 (1965).
- ²J. J. Hopfield, D. G. Thomas, and R. T. Lynch, *Phys. Rev. Lett.* **17**, 312 (1966).
- ³G. W. Iseler and A. J. Strauss, *J. Lumin.* **3**, 1 (1970).
- ⁴T. Fukushima and S. Shionoya, *Jpn. J. Appl. Phys., Part 1* **12**, 549 (1973).
- ⁵A. Naumov, H. Stanzl, K. Wolf, S. Lankes, and W. Gebhardt, *J. Appl. Phys.* **74**, 6178 (1993).
- ⁶I. K. Sou, K. S. Wong, Z. Y. Yang, H. Wang, and G. K. L. Wong, *Appl. Phys. Lett.* **66**, 1915 (1995).
- ⁷A. C. Aten and J. H. Haanstra, *Phys. Lett.* **11**, 97 (1964).
- ⁸A. C. Aten, J. H. Haanstra, and H. de Vries, *Philips Res. Rep.* **20**, 395 (1968).
- ⁹J. D. Cuthbert and D. G. Thomas, *J. Appl. Phys.* **39**, 1573 (1968).
- ¹⁰G. W. Iseler and A. J. Strauss, *J. Lumin.* **3**, 1 (1970).
- ¹¹D. M. Roessler, *J. Appl. Phys.* **41**, 4589 (1970).
- ¹²J. S. Lewis, P. D. Rack, and P. H. Holloway, *J. Cryst. Growth* **184/185**, 1175 (1998).
- ¹³P. D. Rack, P. H. Holloway, W. Park, B. K. Wagner, and C. J. Summers, *J. Appl. Phys.* **84**, 3676 (1998).
- ¹⁴P. D. Rack, P. H. Holloway, W. Park, B. K. Wagner, J. Penczek, C. S. Summers, W. L. Warren, and K. Vanheusden, *Proceedings of the Second International Conference on the Science and Technology of Display Phosphors*, San Diego, CA, Society for Information Display, Nov. 1996, p. 267.
- ¹⁵P. D. Rack, A. Naman, S. Sun, T. Nguyen, K. Jones, and P. H. Holloway, *Proceeding of the Eight International Conference on EL* (W&T Publishing, Berlin, 1996), pp. 355–358.